Finite Element Method Approach to MRAM Modeling

M. Bendra [1], J. Ender [1,2], S. Fiorentini [1], T. Hadamek [1], R.L. de Orio [2],
W. Goes [3], S. Selberherr [2], and V. Sverdlov [1]
[1] Christian Doppler Laboratory for Nonvolatile Magnetoresistive Memory and Logic at the
[2] Institute for Microelectronics, TU Wien, Gußhausstraße 27-29, 1040 Vienna, Austria
[3] Silvaco Europe Ltd., Cambridge, United Kingdom
e-mail bendra@iue.tuwien.ac.at

***Abstract* - Spin-transfer torque magnetoresistive random access memory (STT-MRAM) is among the most promising candidates for emerging memories. Thus, reliable simulation tools are mandatory to provide an important aid for understanding and improving the design of such devices. In this work we are concerned with the simulation of STT-MRAM. The well-known Landau-Lifshitz-Gilbert (LLG) equation describes the magnetization dynamics. Since we are dealing with STT-MRAM, an additional torque term must be added to the LLG equation. The torque acting on the magnetization is generated by the nonequilibrium spin accumulation due to the electric current flowing through the structure. The partial differential LLG equation with the additional torque computed from the spin accumulation is solved using the highly efficient finite element method (FEM). We implemented several time integration schemes using an open-source FEM library. In order to verify and calibrate the FEM implementation, we compared it to a finite difference method (FDM) implementation used as a reference. By properly tailoring the time integration scheme and the time step size, almost identical simulation results as with the FDM are achieved. Proper calibration is essential in order to simulate a more realistic multi-layer structure with a composite switching layer consisting of ferromagnetic layers separated by nonmagnetic buffers.**

Keywords* - *Micromagnetics, STT-MRAM, LLG, spin-transfer torque, finite element method

I. INTRODUCTION

Spin-transfer torque magnetoresistive random access memory (STT-MRAM) is an emerging nonvolatile memory. Magnetic tunnel junctions (MTJ) are the basic means of storing the information of a single bit in every MRAM cell. Since the information must be read and written multiple times and the magnetization in the MTJ changes frequently, the dynamic behavior of this process is of great interest. Here, micromagnetic simulations offer deeper insights. Our goal is to develop a C++ open-source FEM based industry-exploitable modeling and simulation TCAD tool. By implementing our tool on top of the existing FEM library MFEM [1], we can efficiently perform simulations of the magnetization dynamics of spintronic devices. In particular, we are aiming at ultra-scaled MRAM cells with shape-induced perpendicular anisotropy [2]. In these structures, an elongated recording layer consists of several ferromagnetic nanocylinders separated by a nonmagnetic, typically MgO-based, buffer layer needed to boost the perpendicular anisotropy even further [2]. As the magnetization along the recording layer is highly nonuniform due to the formation and propagation of a domain wall, a generalized approach to evaluate the torques based on the fully coupled spin-charge-magnetization dynamics must be considered. The main advantage of a FEM implementation is the possibility to exploit complex nonuniform meshes for discretizing the set of equations without the loss of performance usually experienced within a finite difference approach on refined meshes. The focus of this work is on the calibration and calculation of the demagnetization field as well as comparing several schemes for the time integration of the equations describing the magnetization dynamics.

II. MAGNETIZATION DYNAMICS

To ensure understanding as well as improving STT-MRAM, simulations are an important and reliable supporting aid. In solid state-physics, the LLG equation describes the behavior of the magnetic moments of a ferromagnetic material in an effective magnetic field. In order to be able to describe the dynamics of the magnetization in STT-MRAM, the LLG equation must be supplemented by an additional spin-transfer torque term, which leads to the following equation:

$$\frac{\partial \mathbf{m}}{\partial t} = -\gamma\mu_0\,\mathbf{m}\times\mathbf{H_{eff}} + \alpha\mathbf{m}\times\frac{\partial \mathbf{m}}{\partial t} + \frac{1}{M_S}\mathbf{T_S} \quad (1)$$

$\mathbf{m}=\mathbf{M}/M_S$ is the position-dependent normalized magnetization, M_S is the saturation magnetization, α is the Gilbert damping constant, γ is the gyromagnetic ratio, μ_0 is the vacuum permeability, and $\mathbf{H_{eff}}$ is the effective field which includes different contributions, namely the external field, the anisotropy field, the exchange field, and the demagnetization field.

Modeling the switching of STT-MRAM can be performed by assuming a Slonczewski-like torque expression $\mathbf{T_S}$ [3]. By calculating the nonequilibrium spin accumulation $\mathbf{S}$ over the entire structure and solving the spin and charge drift diffusion equations [4][5], the torque is described by the following expression:

$$\mathbf{T_S} = -\frac{D_e}{\lambda_j^2}\mathbf{m}\times\mathbf{S} - \frac{D_e}{\lambda_\varphi^2}\mathbf{m}\times(\mathbf{m}\times\mathbf{S}) \quad (2)$$

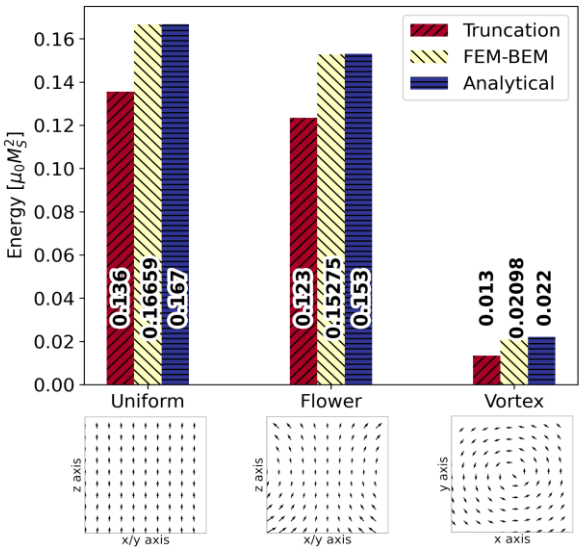

Figure 1. Comparison of the demagnetization energy of a unit cube with different magnetization configurations calculated with the truncation approach and the hybrid FEM-BEM approach.

Here, λ_J is the exchange length, λ_φ is the spin dephasing length, and D_e is the electron diffusion coefficient in the ferromagnetic layers. If an electric current flows through the structure, the spin accumulation is generated. To calculate **S**, the coupled spin and charge transport equations must be solved. In particular, it must be considered that the cells in STT-MRAM devices are based on MTJs, sandwiches of two ferromagnets separated by a tunnel barrier.

III. Demagnetization Field Calculation

The partial differential LLG equation with the additional torque calculated from the spin accumulation is solved using the finite element method (FEM), in which the calculation of the demagnetization field is the most computationally demanding task as it must account for the long-range dipole interaction of magnetic moments. For convenience, the problem of evaluating the demagnetization field can be formulated using the magnetostatic potential which satisfies zero boundary conditions at infinity. For this reason, a large computational domain around the magnetic materials is required. Some approaches to this so-called open boundary problem are described in [6][7].

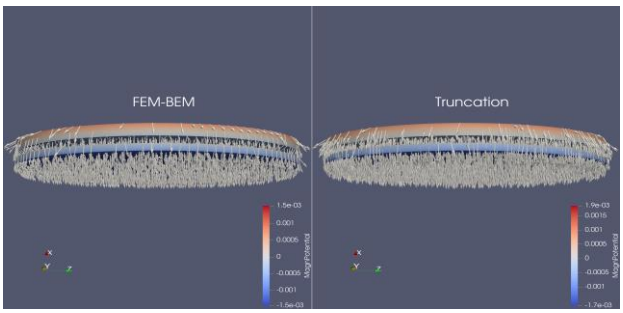

Figure 2. Comparison of the demagnetization field and magnetic potential of an STT-MRAM cell for the parallel magnetization configuration. Arrows indicate the demagnetization field, color-coding represents the magnetic potential.

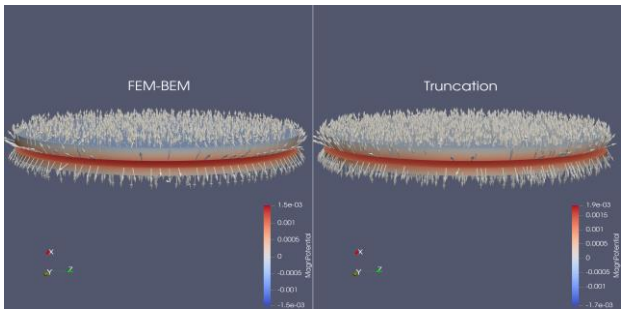

Figure 3. Comparison of the demagnetization field and magnetic potential of an STT-MRAM cell for the anti-parallel magnetization configuration. Arrows indicate the demagnetization field, color-coding represents the magnetic potential.

Since open boundary problems require an infinitely large simulation domain, a domain truncation is required in practice. This approach is referred to as the truncation approach. The accuracy of the calculations depends on the size of the truncated external computational domain surrounding the magnetic material at a certain distance. It has been shown that the external domain should be about five times larger than the magnetic domain to achieve a reasonable accuracy at acceptable computation costs [8].

Alternatively, one can evaluate the magnetostatic potential only in the magnetic domain. For this purpose, the Poisson equation is solved in the magnetic domain, while the behavior of the potential at infinity is guaranteed by the potential of a double layer put on the boundary of the domain. The potential of the double layer is added to the solution of the Poisson equation within the magnetic domain allowing to compute the demagnetization field with high accuracy with reduced computational effort. Within this hybrid approach, the computation is restricted to the magnetic domain where the FEM is coupled to the boundary element method (BEM) [9].

Using these approaches as well as known analytical results, the demagnetization energies of several magnetization configurations considered as standard problems in micromagnetic calculations [10] are compared. These magnetization states are a uniform magnetization state, a flower state, and a vortex-like magnetization state, shown at the bottom of Figure 1. Demagnetization energies computed by the truncation method as well as by the FEM-BEM approach for multiple magnetization states are shown in Figure 1 together with the analytical values. Figure 1 confirms that for a similar mesh in the magnetic domain the hybrid FEM-BEM approach is superior to the truncation approach with respect to accuracy and computational efforts. Since the hybrid FEM-BEM approach gives a very good approximation, we can now proceed to evaluating the demagnetization field of a realistic STT-MRAM cell consisting of several layers. This cell has a diameter of 40nm and consists of two nonmagnetic contacts with a length of 50nm, a ferromagnetic reference layer of 1nm, a free ferromagnetic layer of 1.7nm and a tunnel barrier of 1nm. In this case, the geometry of the magnetic domain is disconnected as it consists of the two ferromagnetic layers separated by a tunnel barrier. To ensure that the hybrid FEM-BEM approach provides a correct solution, the truncation approach is again used for comparison. Figure 2 and Figure 3 show the demagnetization field of an STT-

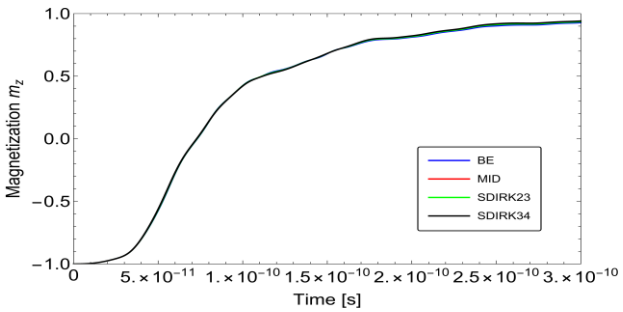

Figure 4. Comparison of all four methods with a time step size of $0.2 \cdot 10^{-12}$ s for the anti-parallel to parallel switching.

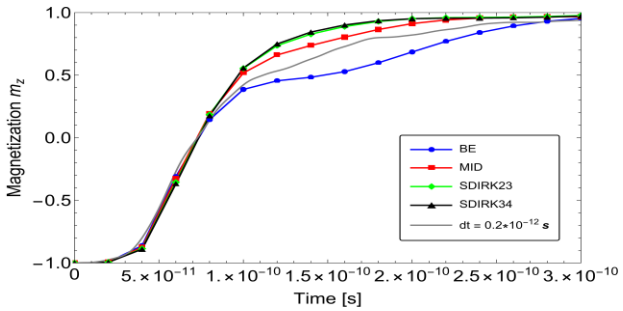

Figure 5. Comparison of all four methods with a time step size of $0.2 \cdot 10^{-10}$ s for the anti-parallel to parallel switching.

MRAM cell for the parallel (P) and for the anti-parallel (AP) configuration, respectively. To better visualize the demagnetization field, the two nonmagnetic contacts and the tunnel barrier are hidden. We can see that both methods give similar results. Therefore, we confirm that the FEM-BEM based approach to evaluate the demagnetization field is implemented correctly in the case of disconnected magnetic domains. This opens the way to proceed further and evaluate the demagnetization field in more complex geometries including synthetic antiferromagnets.

IV. Time Integration Methods

Explicit time integration algorithms are easy to implement and parallelize, and they require a modest amount of computer memory. However, the time step is usually very small and should not exceed a certain value. Otherwise, the integration scheme will become unstable and produce meaningless results. The lack of stability is the price to pay for the algorithmic simplicity of explicit schemes. Implicit schemes are stable, but designing an efficient implicit algorithm is particularly difficult when the underlying partial differential equation and/or discretization procedure are nonlinear. The evaluation load per time step may become heavy compared to that of an explicit scheme, although the time step can be made significantly larger. Moreover, programming implicit-iterative solvers is time consuming, and their efficiency depends on various parameter settings, e.g., stopping criteria. On the other hand, most implicit schemes are unconditionally stable, and the use of large time steps makes it possible to reach the final time faster than with an explicit scheme. Of course, it should be remembered that the accuracy of the time discretization and the convergence behavior of iterative solvers also depend on the time stepping strategy. For this reason, we focus on implicit methods. Below, the four tested methods are introduced, namely the Backward Euler method (BE), the Mid-Point scheme (MID), the two stage, singly diagonal implicit Runge-Kutta method of order three (SDIRK23), and the three stage, singly diagonal implicit Runge-Kutta method of order four (SDIRK34).

The methods are formally described by the equations (3) to (5) [1]:

$$y_{n+1} = y_n + hf\left(t_{n+1}, y_{n+1}\right) \tag{3}$$

$$y_{n+1} = y_n + hf\left(t_n + \frac{h}{2}, \frac{y_n + y_{n+1}}{2}\right) \tag{4}$$

$$y_{n+1} = y_n + h\sum_i b_i k_i \tag{5a}$$

$$k_i = f\left(t_n + c_i h, y_n + h\sum_i a_{ij} k_i\right) \tag{5b}$$

The four different methods can be derived from the general implicit Runge-Kutta equation (5a) and (5b) using appropriate Butcher tables [1]. Figure 4 shows that all methods deliver almost identical results, when the time step is chosen sufficiently small. However, if the time step increases, the difference between the magnetization trajectories becomes larger, as shown in Figure 5. Here, the advantage of higher order schemes becomes apparent as they deliver results close to those at smaller time steps. However, the higher accuracy comes at a much higher computational cost per time step, which can be seen in Figure 6. The upper plot reports the average time required per time step for each method to model the time evolution of the magnetization, while the plot below is the calculation time to simulate the dynamics within 2ns. Obviously, the higher order integration schemes are more computationally demanding, and an accurate tradeoff between achieving a higher accuracy and reducing simulation time is required depending on a particular goal. The MID scheme is the best compromise between accuracy and calculation effort.

V. Comparison of Finite Difference Method and Finite Elemente Method

After carefully calibrating the demagnetization field and choosing a time integration method and a suitable time step, we can verify the switching behavior of STT-MRAM cells simulated with the FEM-BEM implementation by comparing it with a finite difference method (FDM) based numerical solution of the LLG equation.

We consider solving the LLG equation with the Slonczewski anti-damping torque [11]:

$$\frac{\partial \mathbf{m}}{\partial t} = -\gamma\mu_0\, \mathbf{m} \times \mathbf{H_{eff}} + \alpha \mathbf{m} \times \frac{\partial \mathbf{m}}{\partial t} - \frac{\gamma_0 \hbar J_e G(\mathbf{m}\cdot\mathbf{p}, P)}{e\mu_0 M_S d}\, \mathbf{m} \times (\mathbf{m} \times \mathbf{p}) \tag{7}$$

$\hbar$ is the reduced Planck constant, J_e is the current density, d is the thickness of the free layer, and $\gamma_0 = -\gamma\mu_0$ is the rescaled gyromagnetic ratio. The coefficient G describes the dependence of the torque on the interface spin current polarization P and the relative magnetization orientations $\mathbf{m}$ and $\mathbf{p}$ in the free and fixed layers, respectively. Figure 7 shows the time evolution of the average magnetization of the free layer during switching from the anti-parallel to parallel configuration. The parameters used for the magnetic layers in the simulations are summarized in Table I. For the FEM, the meshes are generated using the automatic 2D and 3D tetrahedral mesh generator

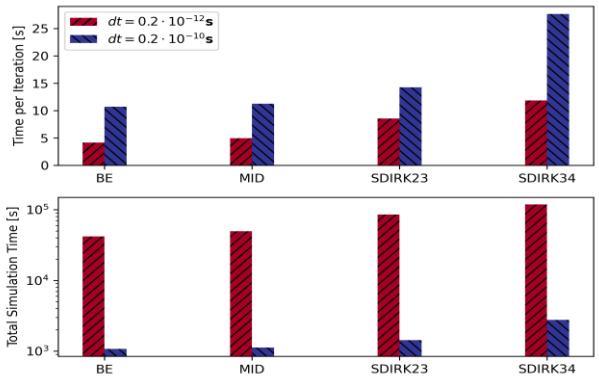

Figure 6. Upper panel: Average time required per time step, for different integration schemes. For a coarser time step, the number of iterations (and the time) grows. Lower panel: Simulation time to model 2ns dynamics with respective time integration schemes.

NETGEN [12]. In order to compare them with our in-house FDM, we chose the FDM mesh as a regular cuboid mesh. The results show a good agreement between the FDM and FEM simulations, confirming the accuracy and reliability of the implemented FEM solver in computing the magnetization dynamics in an MTJ structure.

VI. Conclusion

We demonstrated an open-source FEM based industry-exploitable modeling and simulation TCAD tool for accurate design of emerging MRAM using a modular FEM library (MFEM) [10] implementation to solve the partial differential Landau-Lifshitz-Gilbert equation describing the magnetization dynamics under an external electric current in a multi-layer magnetic structure. The corresponding torques are evaluated by solving the magnetization-dependent, coupled charge and spin transport. We demonstrated that the demagnetization field computed by the truncation method and by the hybrid FEM-BEM approach is identical in a magnetic multi-layer structure. We implemented several time integration schemes. From the above analysis, it can be concluded that the MID scheme is the best compromise between sufficient accuracy and low computational costs. In order to verify the FEM implementation, we compared it to an FDM simulation used as a reference. By properly tailoring the time integration scheme and the time step we demonstrated an almost identical switching in both methods. The proper calibration and verification of the FEM-BEM based LLG solver is essential to simulate a realistic MRAM cell consisting of a fixed, pinned, and a composite free layer separated by nonmagnetic spacers and tunnel barriers.

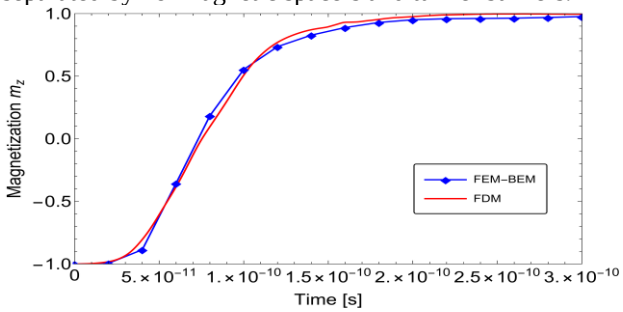

Figure 7. Comparison of FDM to FEM-BEM for the anti-parallel to parallel switching.

TABLE I. Simualtion Parameters

Parameter	*Value*
Gilbert damping, α	0.02
Gyromagnetic ratio, γ	$1.76 \cdot 10^{11}$ rad s^{-1} T^{-1}
Vacuum permeability, μ_0	$4\pi \cdot 10^{-7}$ H m^{-1}
Saturation magnetization, M_S	$8 \cdot 10^{5}$ A m^{-1}
Exchange constant, A	$1.3 \cdot 10^{-11}$ J m^{-1}
Anisotropy constant, K	$2 \cdot 10^{5}$ J m^{-3}
Current spin polarization, β_σ	0.9
Diffusion spin polarization, β_D	1.0
Electron diffusion coefficient, D_e	$2 \cdot 10^{-4}$ m^2/s
Spin-flip length, λ_{sf}	10 nm
Spin dephasing length, λ_φ	5 nm
Exchange length, λ_J	0.5 nm

Acknowledgment

The financial support by the Austrian Federal Ministry for Digital and Economic Affairs, the National Foundation for Research, Technology and Development and the Christian Doppler Research Association is gratefully acknowledged.

References

[1] T. Kolev, V. Dobrev, "MFEM: Modular Finite Element Methods Library," http://mfem.org, 2010.

[2] B. Jinnai, J. Igarashi, K. Watanabe,T. Funatsu, H. Sato, S. Fukami, H. Ohno, "High-Performance Shape-Anisotropy Magnetic Tunnel Junctions down to 2.3 nm," *IEEE International Electron Devices Meeting (IEDM)*, pp. 24.6.1-24.6.4, 2020

[3] J. C. Sloczewski, "Currents, Torques, Polarization Factors in Magnetic Tunnel Junctions," *Physical Review B*, vol. 71, p. 024411, 2004.

[4] C. Abert, M. Ruggeri, F. Bruckner, C. Vogler, G. Hrkac, D. Praetorius, *et al.*, "A Three-Dimensional Spin-Diffusion Model for Micromagnetics," *Scientific Reports*, vol. 5, p. 14855, 2015.

[5] S. Lepadatu, "Unified Treatment of Spin Torques using a Coupled Magnetisation Dynamics and Three-Dimensional Spin Current Solver," *Scientific Reports*, vol. 7, p. 12937, 2017.

[6] X. Brunotte, G. Meunier, J.-F. Imhoff, "Finite Element Modeling of Unbounded Problems using Transformations: a Rigorous, Powerful and Easy Solution," *IEEE Transactions on Magnetics*, vol. 28, no. 2, pp. 1663-1666, 1992.

[7] F. Henrotte, B. Meys, H. Hedia, P. Dular, W. Legros, "Finite Element Modelling with Transformation Techniques," *IEEE Transactions on Magnetics*, vol. 35, no. 3, pp. 1434-1437, 1999.

[8] Q. Chen, A. Konrad, "A Review of Finite Element Open Boundary Techniques for Static and Quasi-Static Electromagnetic Field Problems," *IEEE Transactions on Magnetics*, vol. 33, no. 1, pp. 663-676, 1997.

[9] D. R. Fredkin, T. R. Koehler, "Hybrid Method for Computing Demagnetizing Fields," *IEEE Transactions on Magnetics*, vol. 26, no. 2, pp. 415-417, 1990.

[10] C. Abert, L. Exl, G. Selke, A. Drews, T. Schrefl, "Numerical Methods for the Stray-Field Calculation: A Comparison of Recently Developed Algorithms," *Journal of Magnetism and Magnetic Materials*, vol. 326, pp. 176-185, 2013.

[11] C. Abert, "Micromagnetics and Spintronics: Models and Numerical Methods," *The European Physical Journal B*, vol. 92, no. 6, pp. 1-45, 2019.

[12] J. Schöberl, "NETGEN An Advancing Front 2D/3D-Mesh Generator Based on Abstract Rules," *Computing and Visualization in Science*, vol. 1, pp. 41-52, 1997.